Microporous and Mesoporous Materials 198 (2014) 1–8

Contents lists available at ScienceDirect

Microporous and Mesoporous Materials

journal homepage: www.elsevier.com/locate/micromeso

Exploration of room temperature synthesis of palladium containing cubic MCM-48 mesoporous materials

Harrison S. Kibombo, Vagulejan Balasanthiran, Chia-Ming Wu, Rui Peng, Ranjit T. Koodali *

Department of Chemistry, University of South Dakota, Vermillion, SD 57069, USA

ARTICLE INFO

Article history:
Received 19 February 2014
Received in revised form 7 April 2014
Accepted 10 July 2014
Available online 18 July 2014

Keywords:
Pd-MCM-48
Cubic phase
Mesoporous
Palladium
Hydrogenation

ABSTRACT

Pd-MCM-48 mesoporous materials were synthesized by a modified Stöber synthesis method in 4 h at room temperature. Pd nanoparticles were prepared by using $Na_2[PdCl_4]$ and $Pd(acac)_2$ as Pd precursors, and their influence in the preparation of the cubic MCM-48 mesoporous phase was investigated. In addition, Pd(0) nanoparticles was prepared separately and added to the synthesis gel. The influence of varying the Pd precursor, solvent media, the time of addition of Pd precursor, and the concentration of $NaBH_4$ reducing agent used for preparation of Pd(0) and its effect for the formation of the cubic phase were investigated. These resultant materials were characterized by powder X-ray diffraction (XRD), transmission electron microscopy (TEM), UV–Visible spectroscopy, nitrogen physisorption, and CO-Pulse titration. Reusability studies assessing a material prepared using Pd(0)-DMAP encapsulated nanoparticles that were reduced with 0.1 N $NaBH_4$ *i.e.* 3%Pd-MCM-48-D-N01 indicate that the yields for the hydrogenation of *trans*-cinnamic acid are greater than 95% even after 8 catalytic cycles, and at which the cubic phase was maintained under our experimental conditions.

1. Introduction

MCM-48 material is one of the M41S class of materials, and is postulated to be an effective support for several catalytic applications due to their three-dimensional bi-continuous network of pore structures that provide efficient molecular trafficking. In general, MCM-48 based catalysts possess enhanced activity compared with other uni-dimensional supports such as MCM-41 materials. However the synthesis of the cubic phase MCM-48 materials is tedious and can often take several days [1,2]. A rapid and simple MCM-48 synthesis at room temperature in 30 min has been reported by us previously [3].

Metal supported catalysts have been extensively employed successfully in catalysis, adsorption, bio-molecular purification, and drug delivery applications due to their high activity and reusability. Considerable research efforts have focused on the development of environmental friendly and metal supported heterogeneous catalysts prepared by the incorporation of the active catalytic species onto supported materials such as polymers [4] and porous materials such as SiO_2 [5,6], and mesoporous materials like MCM-41 [7], SBA-15 [8], and MCM-22 [9].

Mesoporous silica has been the support material of choice due to its relatively high surface area, uniform pore size, and large pore volume that facilitate better dispersion of the catalytically active species. A high thermally stable model catalytic system of Pt core coated with mesoporous SiO_2 ($Pt@SiO_2$) has been reported by Joo et al. [6]. Highly monodispersed silica nanoparticles using self-assembled organometallic spheres as endo-templates has been reported by Suzuki et al. [10].

Several research groups have studied hydrogenation reactions using Pd-MCM-41 [11], Pd on MCM-48 [12], and Pd-SiO_2 [13]. Pd supported on mesoporous materials MCM-41, MCM-48, and SBA-15 etc. have been synthesized. Among the various periodic mesoporous supports examined for dispersion of Pd nanoparticles, MCM-41 has been a popular choice because of its relative ease of preparation compared to the cubic MCM-48 phase. The cubic phase is extremely sensitive to small variations in experimental conditions and this has precluded the wide scale applicability of MCM-48 materials. Thus, literature studies containing Pd nanoparticles dispersed in MCM-48 matrix are scare [14,15] and furthermore some methods reported are complicated and not easily accessible such as magnetron sputtering [16] or require tedious [17] and long preparation time of 72 h at temperatures >100 °C [18,19]. In this work, our goal was to develop a reliable and simple procedure for preparing Pd-MCM-48 materials. Furthermore, it is attractive to prepare these materials at room temperature and using relatively low amounts of surfactants, for large scale applications. In this study, we investigated the influence of varying the Pd precursor, the time of addition of Pd precursor, and the

* Corresponding author. Tel.: +1 605 677 6189; fax: +1 605 677 6397.
E-mail address: Ranjit.Koodali@usd.edu (R.T. Koodali).

http://dx.doi.org/10.1016/j.micromeso.2014.07.012
1387-1811/

concentration of $NaBH_4$ reducing agent used for preparation of Pd(0) on the formation of the cubic MCM-48 phase since these have a profound effect on the resulting mesoporous phase that is formed. The mesoporous materials were characterized by powder X-ray diffraction (XRD), transmission electron microscopy (TEM), UV–Visible spectroscopy, nitrogen physisorption, and CO-Pulse titration. Subsequently, we evaluated the reusability of the materials using hydrogenation of *trans*-cinnamic acid as a model reaction. This work provides practitioners in heterogeneous catalysis with a facile method for the preparation of Pd-MCM-48 catalysts that may be applied to regio- and chemoselective hydrogenation [20], hydrocarboxylation [21], carbonylation [22], oxidation [8], etherification [23], hydrogenolysis of ethers [12], reduction of functional containing organic molecules, and in coupling reactions such as Suzuki, and Heck.

2. Experimental section

2.1. Chemicals used

Dimethylaminopyridine (DMAP, 99%, Acros), toluene (Acros), tetra-*n*-octylammonium bromide (TOABr, 98 + % Alfa Aesar), sodium borohydride (98% Acros) and sodium sulfate anhydrous powder (Fisher) were used as received for the synthesis of Pd(0) nanoparticles. Cetyltrimethylammonium bromide (CTAB, 99+%, Acros), ethanol (absolute 200 Proof, AAPER), aqueous ammonia (Fisher), tetraethoxysilane (99%, Alfa Aesar), palladium(II) 2,4-pentanedionate (Alfa Aesar), and sodium tetrachloropalladate(II) (Pressure Chemicals) were used as received.

2.2. Synthesis of Pd(0) nanoparticles

Pd(0) nanoparticles were synthesized by the reduction of $Na_2[PdCl_4]$ using $NaBH_4$ and stabilized by TOABr as a capping agent. In this synthesis, 9.6 mL of a 47 mM aqueous solution of $Na_2[PdCl_4]$ was mixed with 40 mL of a 50 mM solution of TOABr dissolved in toluene, and stirred at 300 rpm for 15 min. A red–brown organic solution and a colorless aqueous phase was observed due to the complete transfer of $Na_2[PdCl_4]$ to the organic phase. The colorless aqueous phase was separated and the toluene phase was dried with Na_2SO_4. Then, 11.4 mL of a freshly prepared 0.1–1.0 N $NaBH_4$ aqueous solution was added drop wise for a period of 2 h under vigorous stirring. The mixture was stirred overnight, then washed with 40 mL of a 0.1 M H_2SO_4 aqueous solution, 40 mL of a 0.1 N NaOH aqueous solution, and 40 mL of water respectively. Finally the organosol was dried over anhydrous Na_2SO_4.

0.1 M 4-dimethylaminopyridine (DMAP) solution (10 mL) was used as a phase transfer agent and was prepared by dissolving 0.1 g of DMAP in 10 mL of deionized water. Then, aqueous DMAP solution was added to 40 mL of the as-synthesized Pd nanoparticles in toluene. The mixture was stirred for 2 h to complete the transfer of the Pd nanoparticles to the aqueous phase.

2.3. Synthesis of MCM-48 mesoporous materials

2.3.1. Synthesis of Si-MCM-48 mesoporous materials

Si-MCM-48 materials were synthesized using a modified Stöber synthesis. In a typical synthesis, 50 mL of deionized water, 25 mL of ethanol, 1.2 g (3.3 mmol) of CTAB, 6 mL of aq. NH_3 (0.09 mol), and 1.8 mL (8 mmol) of tetraethylorthosilicate (TEOS) were sequentially added to a polypropylene bottle (125 mL) and stirred for 4 h at a rate of 300 rpm. The composition of the initial siliceous gel is 0.41 CTAB: 11 aq. NH_3: 1.0 TEOS: 53 Ethanol: 344 H_2O. After 4 h, the mesoporous material obtained was washed extensively with deionized water. The materials were dried overnight in an oven at 100 °C. The dried material was ground well and calcined at 550 °C (heating rate of 3 °C per minute) for 6 h in order to remove the surfactant molecules.

2.3.2. Synthesis of Pd-MCM-48 mesoporous materials by direct synthesis

Pd-MCM-48 materials were synthesized using a modified Stöber synthesis. Typically, 50 mL deionized water, an appropriate amount of Pd precursor required for the desired loading, 25 mL ethanol, 1.2 g (3.3 mmol) of CTAB, 6 mL of aq. NH_3 (0.09 mol) and 1.8 mL (8 mmol) of tetraethylorthosilicate (TEOS) were sequentially added to a polypropylene bottle (125 mL) and stirred for 4 h at a rate of 300 rpm. The composition of the initial siliceous gel is 0.41 CTAB: 11 aq. NH_3: 1.0 TEOS: 53 Ethanol: 344 H_2O. The amount of palladium in the synthesis gel was varied by changing the amount of Pd precursor. After 4 h, the mesoporous material was washed extensively with deionized water. Pd-MCM-48 materials were prepared using three different Pd precursors: (i) $Na_2[PdCl_4]$, (ii) $Pd(acac)_2$, and (iii) Pd(0)-DMAP encapsulated nanoparticles and are denoted as Pd-MCM-48-NP, Pd-MCM-48-A, Pd-MCM-48-D respectively. The materials were dried overnight in an oven at 100 °C. The dried materials were ground well using a mortar and pestle and calcined at 550 °C (heating rate of 3 °C per minute) for 6 h.

2.3.3. Synthesis of Pd-MCM-48 by Post Impregnation Method

Pd was deposited by post impregnation method to produce Pd-MCM-48-PI materials for comparison with the direct synthesis. In this method, calcined Si-MCM-48 was impregnated with aqueous or ethanolic solvents of three different Pd precursors: (i) $Na_2[PdCl_4]$, (ii) $Pd(acac)_2$, and (iii) Pd(0)-DMAP encapsulated nanoparticles. The appropriate amount of Pd precursor was dissolved in 15 mL EtOH and 5 mL water. Then the solution was added to the Si-MCM-48, stirred for 2 h at 300 rpm. The resulting composition was dried in an oven set at 100 °C. The dried materials were calcined at 550 °C (ramp rate of 3 °C per minute) for 6 h.

The calcined Pd-MCM-48 contains Pd in the 2+ oxidation state. Hence they were reduced in hydrogen flow (20 mL/min) at 300 °C for 2 h in a tubular furnace.

2.4. Characterization techniques

UV–Vis spectra of the Pd(0) nanoparticles and Pd precursors were recorded in the wavelength range of 200–800 nm with a Cary 100 Bio UV–Visible spectrometer. DMAP solution was used as a reference for the Pd nanoparticles and water was used as a reference for $Na_2[PdCl_4]$. A scan rate of 300 nm/min was typically used for recording the spectra.

Nitrogen physisorption isotherms of Pd-MCM-48 materials were measured at 77 K using a Quantachrome NOVA 2200*e* series instrument. Before the measurements, Pd-MCM-48 samples were degassed extensively under vacuum at 100 ± 10 °C. The Brunauer–Emmett–Teller (BET) equation was used to calculate the surface area from the adsorption data obtained at relative pressure P/P_0 between 0.05 and 0.30. The total pore volume of mesoporous materials were calculated from the amount of nitrogen adsorbed at highest relative pressure ratio $P/P_0 \sim 0.99$. The pore size distribution was calculated by analyzing the N_2 isotherm using the Barrett–Joyner–Halenda (BJH) method and applying it to the desorption isotherm.

Powder XRD patterns were collected by using a Rigaku Ultima IV instrument operated at 1.76 kW (Voltage = 44 kV and Current = 40 mA), and with Cu Kα radiation (λ = 1.5408 Å). The sample was placed on the glass sample holder and then smoothly packed tightly using a glass microscope slide. The low angle regions were scanned from 2° to 6° (2θ) with a step size of 0.02°. Wide angle XRD

measurements were also made for selected mesoporous materials in the 2θ range of 20–75°.

Samples for transmission electron microscopy were prepared by first sonicating ~5 mg Pd-MCM-48 in 25 mL ethanol. One drop of this dispersion was carefully deposited on a carbon coated copper grid (200 mesh). The grid was allowed to dry at room temperature overnight before it was transferred to the sample chamber for TEM studies. TEM images were acquired using a FEI Tecnai G^2 F30 instrument at an accelerating voltage of 200 kV.

The palladium content in the Pd-MCM-48 samples was determined by using a Thermo Jarell Ash atomic absorption spectrophotometer (AAS) as described in the following sections. 0.346 g of $Na_2[PdCl_4]$ was exactly weighed, dissolved in 25 mL of deionized water, and the solution was transferred quantitatively to a 500 mL standard flask and diluted to the mark using deionized water. The concentration of the standard stock solution obtained was 250 ppm. From this stock solution, a series of known concentrations of Pd^{2+} were prepared. The corresponding absorbance of the standard solutions were measured and a calibration graph plotted. A known quantity of Pd-MCM-48 sample (~50–100 mg) was stirred overnight with concentrated HCl. The silica phase was carefully filtered, and the filtrate was quantitatively transferred to a standard flask and diluted to a known volume. These solutions were analyzed for Pd^{2+} using AAS as described previously and the concentrations determined from the calibration plots made previously.

Pulse chemisorption studies were carried out by using ChemBET 3000 instrument. The appropriate amount of Pd-MCM-48 was reduced at 300 °C under hydrogen flow for 2 h prior to CO chemisorption. The sample was allowed to cool to room temperature. Helium gas (90 mL/min) was used as a carrier gas and CO was used as the titrant. The chemisorption measurements were carried out at room temperature by dosing 100 μL pulse of CO until the Pd surface was saturated. Saturation can be inferred when the peak intensity (related to the amount of CO consumption) becomes constant.

Hydrogenation reactions were conducted for *trans*-cinnamic acid using Pd-MCM-48. In a typical catalysis reaction, Pd-MCM-48 catalyst (0.25 g), *trans*-cinnamic acid (0.4 g), nonane (0.1 mL), and ethanol (25 mL) were added to a 100 mL round bottom flask under a constant flow of H_2 (flow rate 20 mL/min) for 30 min. The catalyst was filtered and washed with ethanol (2×5 mL). The filtrate was evaporated to yield the pure hydrogenated product. The products and the yield of the reaction were determined by ^1H NMR spectroscopy. In addition, the reaction mixture was injected into a GC–MS instrument (Shimadzu QP 2100) equipped with a silica column (J&W Scientific, 122-5532, DB-5ms equivalent to a (5% phenyl) methyl polysiloxane, 30 m × 0.25 mm). Confirmation of the product was carried out by Mass Spectrometry. The hydrogenation was also successful under a steady H_2 atmosphere (a balloon filled with H_2).

The reusability of the catalyst was studied to evaluate the recyclability of the Pd catalyst. After the hydrogenation of *trans*-cinnamic acid reaction, the catalyst was filtered and washed with ethanol several times and dried at 100 °C for an overnight. The reaction was then carried out using the recycled catalyst and the yield of the product determined as described previously.

3. Results and discussion

3.1. Powder X-ray diffraction studies

Fig. 1 shows the powder XRD patterns of Pd containing mesoporous materials prepared by adding the required amount of $Na_2[PdCl_4]$ corresponding to 0.25, 1.0, and 3.0 wt.% Pd in the synthesis gel. In this method, we added $Na_2[PdCl_4]$ to the surfactant solution and then added ammonia and TEOS. We can observe that the intensity of the peak at $2\theta < 3°$ for the 0.25 wt.% Pd loading is greater than that of the 1 and 3 wt.%. More importantly, the small shoulder at 2θ near 3.2° which is characteristic of the cubic phase is very weak in the sample containing 1 wt.% Pd and disappears when the loading is increased to 3 wt.%. This indicates that it is more viable to prepare cubic Pd-MCM-48 materials at low loadings (<1 wt.% Pd) only using $Na_2[PdCl_4]$ at room temperature under the experimental conditions in this study. Even though we were successful in synthesizing Pd-MCM-48 at such low loadings, it was challenging to prepare a cubic phase containing higher loadings of Pd.

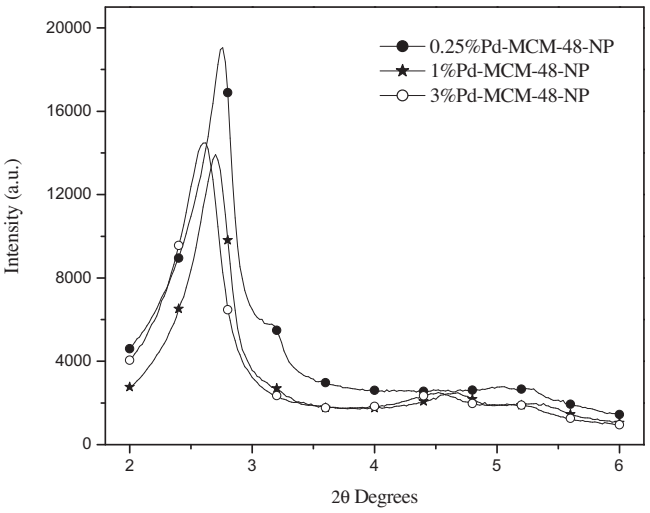

Fig. 1. Powder XRD diffractograms of Pd-MCM-48-NP prepared using $Na_2[PdCl_4]$ with different Pd loadings of 0.25, 1, and 3 wt.%.

We modified our synthetic procedure and added the Pd precursor after the addition of all the remaining components at different times. Fig. 2 shows the XRD diffractograms of Pd-MCM-48-NP where $Na_2[PdCl_4]$, corresponding to 1 wt.% Pd loading, that was added after 20, 30, and 60 min of addition of TEOS to the synthesis gel. The samples labelled, 1%Pd-MCM-48-NP-t20, 1%Pd-MCM-48-NP-t30, and 1%Pd-MCM-48-NP-t60 exhibit patterns similar to wormhole, lamellar, and cubic mesoporous phases respectively. It

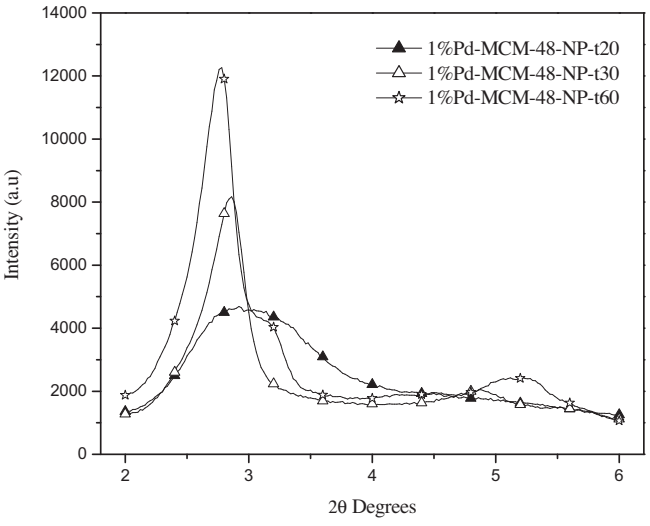

Fig. 2. Powder XRD diffractograms of Pd-MCM-48-NP of 1 wt.%Pd loading prepared by addition of $Na_2[PdCl_4]$ at different time intervals of 20, 30 and 60 min.

is clear that the mesoporous phase obtained is influenced by the time of addition of $Na_2[PdCl_4]$. This may be due to the fact that the interaction between the cationic surfactant (S^+) and the inorganic precursor (I^-) is influenced by the addition of $[PdCl_4]^{2-}$. During the initial stages of the formation of the mesoporous materials, the inorganic precursor, I^- is highly charged and hence the charge density on the surfactant molecule is also very high. Thus, when an anion such as $[PdCl_4]^{2-}$ is added at early stages of the formation of the mesoporous phase, *i.e.* 30 min after addition of TEOS, the interaction between the positively charged surfactant and $[PdCl_4]^{2-}$ is very strong and this leads to the formation of a structure with surfactant packing parameter (g) = 1.0, *i.e.* lamellar phase.

However, when $Na_2[PdCl_4]$ is added at 60 min after the addition of other precursors, the charge density on the silica is significantly lower. In order to match the charge density, the surfactant reorganizes and adopts an appropriate geometry, *i.e.* hexagonal or cubic to match this charge density. Our experimental composition is optimized for the successful preparation of the cubic phase. Thus, a cubic phase is formed when $Na_2[PdCl_4]$ is added later to the synthesis gel. The Pd-MCM-48-NP sample synthesized by adding $Na_2[PdCl_4]$ after 60 min denoted as 1%Pd-MCM-48-NP-t60 yields poor quality of cubic phase and suffers from reproducibility in our experience. These results indicate that the mesoporous phase is influenced by the time of addition of the Pd precursor and that use of $Na_2[PdCl_4]$ to prepare Pd-MCM-48 cubic mesoporous materials at room temperature leads to poor control of the cubic phase.

We also expect that the nature of the Pd precursor may influence the formation of mesoporous phase. In order to study this factor, we used $Pd(acac)_2$ instead of $Na_2[PdCl_4]$ in the synthesis gel. In one experiment, $Pd(acac)_2$ was dissolved in water, heated to 80 °C to solubilize $Pd(acac)_2$, and then added to synthesis gel to obtain 1%Pd-MCM-48-A-H_2O. The XRD patterns in Fig. 3 suggest that our attempts to synthesize the cubic phase using this approach were not very successful due to the limited solubility of $Pd(acac)_2$ in water. We then dissolved $Pd(acac)_2$ in ethanol prior to their addition to the synthesis gel. Using ethanol as the solvent led to the formation of hexagonal phase as indicated in the XRD pattern of 1%Pd-MCM-48-A-EtOH. When $Pd(acac)_2$ is dissolved in small amounts of ethanol, the alcohol molecules penetrate into the surfactant micelles. This results in an increase in the total volume (of the surfactant chain and the co-solvent molecules). This increases the surfactant packing parameter, g and a hexagonal MCM-41 phase is formed as observed previously on addition of small amounts of alcohol in the synthesis gel [24]. However, the use of toluene to dissolve $Pd(acac)_2$ led to the formation of a poor quality cubic phase as exhibited by 1%Pd-MCM-48-A-Tol. The results obtained using the two Pd precursors, Na_2PdCl_4 and $Pd(acac)_2$ suggest that it is fairly challenging to prepare Pd-MCM-48 cubic materials at room temperature. This motivated us to pursue the preparation of Pd-MCM-48 materials using pre-formed Pd(0) nanoparticles. Pd nanoparticle incorporated mesoporous materials have been reported for SBA-15 [25] and post impregnated Pd nanoparticles have been incorporated in MCM-41 and MCM-48 [26]. In our approach, Pd(0) nanoparticles stabilized by DMAP were added instead of $Na_2[PdCl_4]$ or $Pd(acac)_2$. This method also affords the possibility of using Pd(0) nanoparticles of different particle sizes. It has been reported that Pd(0) nanoparticles with varying sizes can be prepared by merely varying the concentration of the reducing agent, *i.e.* using 0.1, 0.5, and 1.0 N $NaBH_4$. The Pd(0) nanoparticles prepared using 0.1, 0.5, and 1 N $NaBH_4$ are labeled as 1%Pd-MCM-48-D-N01, 1%Pd-MCM-48-D-N05 and 1%Pd-MCM-48-D-N1 respectively and the corresponding XRD patterns are shown in Fig. 4.

The XRD patterns of the MCM-48 samples containing Pd(0) nanoparticles prepared using 0.1 N $NaBH_4$ indicate the formation of the cubic MCM-48 phase. In particular, the material prepared using 0.5 N $NaBH_4$ show distinct diffraction peaks due to d_{211}, d_{220}, d_{400}, d_{420}, and d_{332} indicating a high quality of cubic phase belonging to $Ia\bar{3}d$ symmetry. This diffraction pattern is also consistent with the previously reported cubic mesoporous materials [27,28]. Pd samples prepared using 0.1 and 0.5 N $NaBH_4$ show distinct peaks due to the d_{220} plane, which indicates the formation of the cubic material while the sample prepared using 1.0 N $NaBH_4$ does not seem to have formed a good cubic phase. At this moment, the rationale for the formation of the cubic phase by changing the concentration of $NaBH_4$ used to reduce Pd^{2+} ions is still fully unclear and is under investigation since only the particle sizes of Pd(0) are affected by changing its concentration. In addition, AAS studies of these three mesoporous materials indicate Pd loadings of 0.6 ± 0.1 wt.% in the final product. Since, we were successful in the preparation of cubic MCM-48 phase by using Pd(0) nanoparticles reduced using 0.1 N $NaBH_4$, we prepared Pd-MCM-48 materials with different loadings of Pd, *i.e.*1, 2, 3, and 4 wt.% Pd using this condition. The XRD pattern of 1%Pd-MCM-48-D-N01 was also

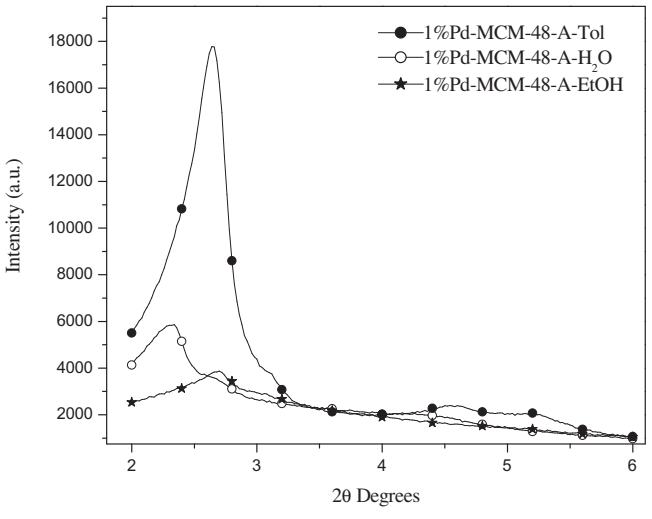

Fig. 3. Powder XRD diffractograms of Pd containing MCM-48 materials synthesized by using $Pd(acac)_2$ precursor dissolved in different media such as toluene, water, and ethanol.

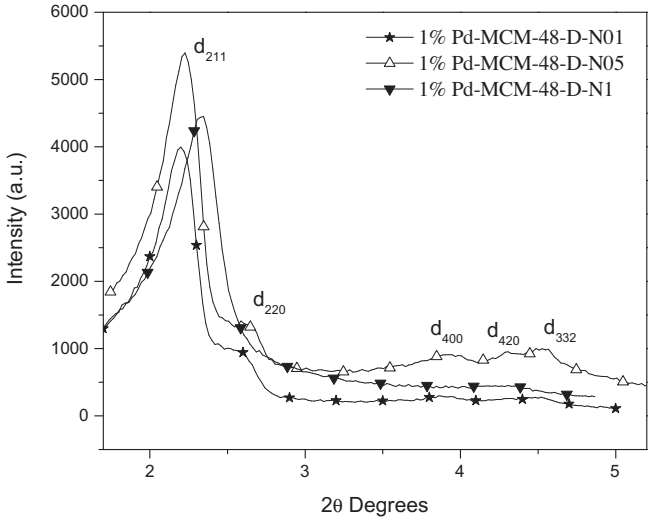

Fig. 4. Low angle powder XRD diffractograms of 1 wt.% Pd loading prepared by addition of Pd(0) nanoparticles that were reduced by different $NaBH_4$ concentrations of 0.1, 0.5 and 1 N.

conducted in the high angle region, i.e. $2\theta = 25–75°$ (not shown). No peaks due to Pd were observed, which indicates high dispersion of Pd species in this material, and this result is consistent with CO chemisorption studies (discussed later in the manuscript). A similar observation was found for the sample with 2% loading of Pd.

A difference in the XRD pattern is observed when the Pd nanoparticle loading is increased to 3 wt.% and above. The high angle diffraction pattern of 3%-Pd-MCM-48-D-N01 shown in Fig. 5 exhibits a peak at 2θ near 33.8° that is attributed to presence of PdO while the peaks near $2\theta = 42°$, 54.8°, 60.7° and 71.4° is due to Pd(0) [29]. A similar result was obtained for the sample prepared containing 4 wt.% Pd(0). The XRD results also suggest that some residual Pd(0) still persists despite their calcination in air to remove the surfactant. Also, AAS studies of the mesoporous materials, containing 2, 3, and 4 wt.% of Pd in the synthesis gel indicate final Pd loadings corresponding to 1.6 ± 0.1, 2.63 ± 0.2, and 3.25 ± 0.2 wt.% respectively.

3.2. UV–Visible spectroscopy

The Pd(0) nanoparticle phase transfer from the organic phase to the aqueous phase can be monitored by UV–Vis spectroscopy. The UV–Vis spectrum (Fig. 6) of $Na_2[PdCl_4]$ exhibits two peaks at 207 and 234 nm. These peaks may be attributed to Ligand to Metal Charge-Transfer (LMCT) transitions from Cl^- to Pd^{2+}. $Na_2[PdCl_4]$ aqueous solution is a pale yellow solution as shown in the inset in Fig. 6. The Pd^{2+} ions are transferred to toluene by using TOABr as a phase transfer agent. The color changed from pale yellow to orange after the phase transfer process. We reduced the Pd^{2+} ions to Pd(0) in toluene phase for controlled reduction of Pd particles by use of $NaBH_4$. This is because the aqueous phase reduction of Pd ions tends to form larger clusters or bigger Pd particles. The UV–Vis spectra of DMAP encapsulated Pd(0) nanoparticle in the aqueous and organic phase (toluene) is shown in Fig. 7. Normally colloidal nanoparticle dispersions of transition metals show bright colors due to the surface plasmon resonance. For Pd, the dielectric constant dictates a resonance in the UV region [30]. DMAP encapsulated Pd(0) nanoparticle in aqueous phase shows a clear absorption band at 309 nm. This absorption band is consistent with the Pd(0)-DMAP (307 nm) peak as reported by Ribera et al. The UV–Vis spectrum of Pd nanoparticles in toluene shows the absence of any distinct peak [31].

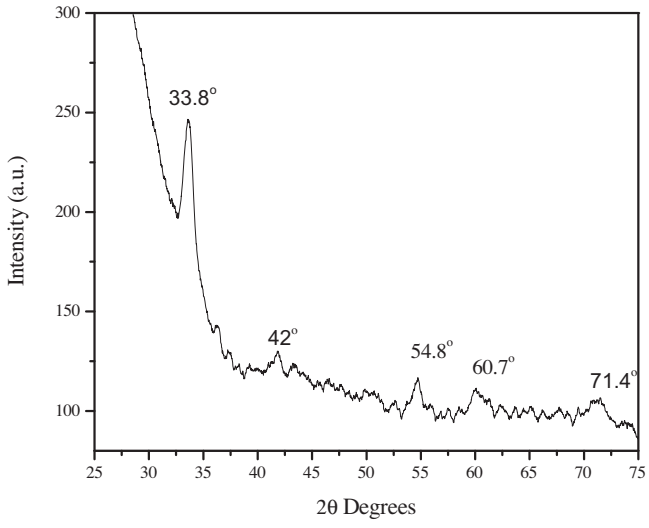

Fig. 5. Wide angle powder XRD pattern of calcined 3%Pd-MCM-48-D-N01 mesoporous material prepared using Pd(0) nanoparticles.

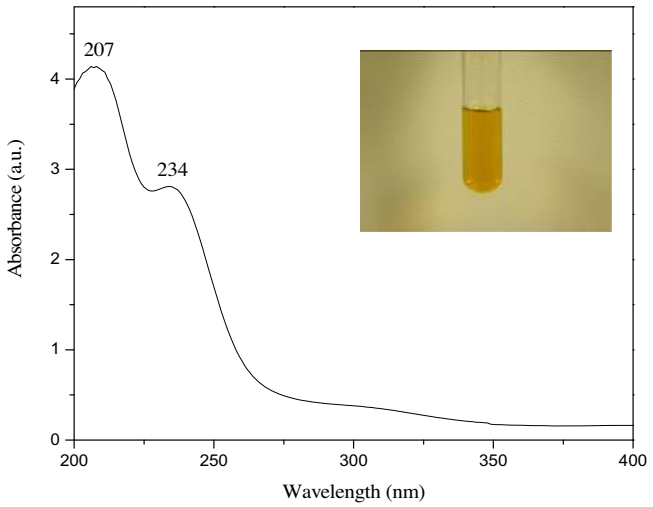

Fig. 6. UV–Vis spectra of 2 mM Na_2PdCl_4 solution.

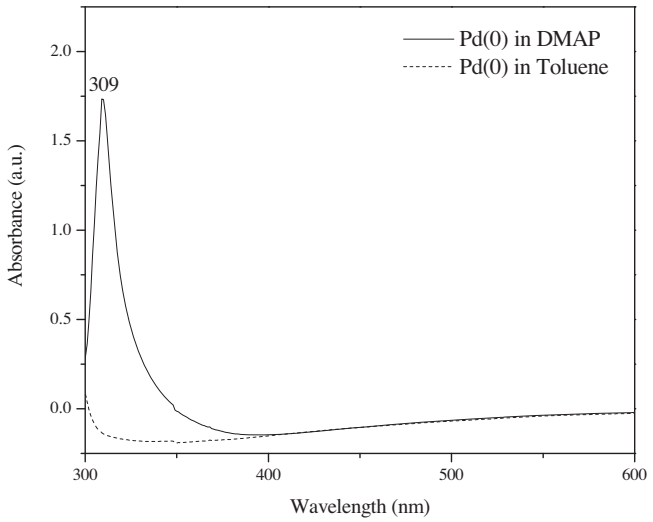

Fig. 7. UV–Vis spectra of Pd(0) nanoparticles in DMAP solution and toluene.

3.3. Nitrogen physisorption studies

The textural properties of Pd-MCM-48 were evaluated. A typical type IV adsorption isotherm (Fig. 8A) is observed for all Pd-MCM-48 materials and for the sake of clarity one representative isotherm is shown. At relative pressures, P/P_0 between 0.2 and 0.4, a sharp inflection due to capillary condensation within the pores is observed, which is characteristic of periodic mesoporous materials. Table 1 provides a comparative summary of textural properties of Pd containing mesoporous materials. The surface area and pore volume of Pd-MCM-48 materials prepared in this study are comparable or larger to values reported previously for Pd containing mesoporous materials suggesting that the room temperature 4 h preparation for the synthesis of MCM-48 materials using pre-formed Pd(0) nanoparticles is an attractive method. The pore size distribution shown in Fig. 8B indicates that the pores are fairly uniform. Table 2 shows the textural property of Pd-MCM-48 materials prepared using various Pd precursors.

A low surface area of 191 m^2/g and a fairly broad pore diameter of 4.9 nm was obtained for 1%-Pd-MCM-48-NP-t20. There is a substantial increase in the surface area when the addition of $Na_2[PdCl_4]$ is delayed to 30 min but a cubic phase was not obtained

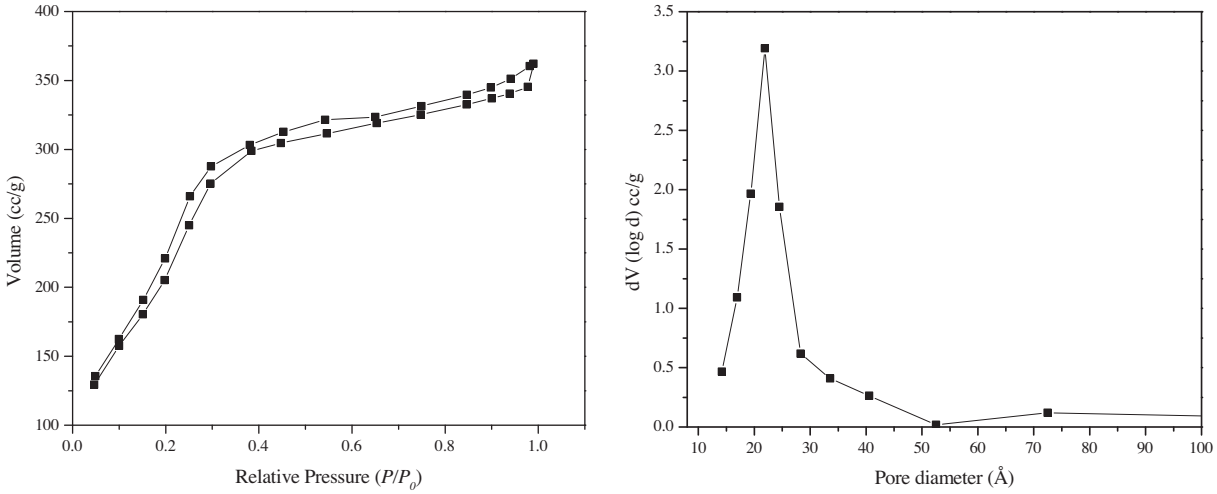

Fig. 8. Nitrogen isotherm of 1%Pd-MCM-48-D-N01 prepared using DMAP encapsulated Pd(0) nanoparticle and reduced using 0.1 N $NaBH_4$.

Table 1
Comparative analysis of surface area, pore size, and pore volume of Pd containing mesoporous materials.

Material	Surface area (m^2/g)	Pore diameter (nm)	Pore volume (cc/g)	Refs.
Pd@MCM-41	897	4.0	0.66	[11]
Pd-TMS11	750	2.61	Not provided	[31]
Pd/SBA-15	662	6.51	1.04	[8]
Pd/MCM-41	1031	2.23	0.73	[26]
Pd/MCM-48	1035	2.43	0.81	[26]
PdKIT-6	357	4.80	0.22	[2]
Pd-MCM-48	800–1900	~2.2	0.8–1.5	Present study

Table 2
Textural properties of Pd containing mesoporous materials prepared using the various methods.

Material	Surface area (m^2/g)[a]	Pore volume (cc/g)[b]	Pore diameter (nm)[c]
1%Pd-MCM-48-NP-t20	191	0.32	4.9
1%Pd-MCM-48-NP-t30	790	0.55	1.7
1%Pd-MCM-48-NP-t60	1900	0.96	2.2
1%Pd-MCM-48-D-N01	1357	0.72	2.2
1%Pd-MCM-48-D-N05	1557	0.82	2.2
1%Pd-MCM-48-D-N1	1546	0.87	1.9
2%Pd-MCM-48-D-N01	1697	0.84	1.9
3%Pd-MCM-48-D-N01	1788	0.94	1.8
4%Pd-MCM-48-D-N01	1575	0.95	1.8
1%Pd-MCM-48-NP-PI	637	0.54	1.7
1%Pd-MCM-48-D-N01-PI	501	0.33	2.0
1%Pd-MCM-48-A-Tol-PI	1360	0.68	1.9

[a] Calculated by using the Brunauer–Emmett–Teller (BET) equation in the relative pressure (P/P_0) range of 0.05–0.35 in the adsorption isotherm.
[b] Calculated from the amount of N_2 adsorbed at the highest relative pressure of (P/P_0) ~ 0.99.
[c] Calculated by applying the Barrett–Joyner–Halenda (BJH) equation for the desorption isotherm.

as discussed previously. However a delay in addition of $Na_2[PdCl_4]$ to the synthesis gel to 60 min results in the material, 1%-Pd-MCM-48-NP-t60 that constitutes a cubic phase with a large surface area of 1900 m^2/g and uniform pore diameter of 2.2 nm. Table 2 also shows the textural properties of Pd-MCM-48 mesoporous materials prepared by addition of Pd(0) nanoparticles prepared using different concentrations of $NaBH_4$. All materials exhibit mesoporous phase with uniform pore size distribution in the range of ~2.2 nm and relatively large surface areas in the range of 1357–1557 m^2/g. The textural properties of Pd-MCM-48-D-N01 materials prepared with different amounts of Pd (1–4 wt.%) were also examined. The pore volume was found to increase from 0.72 to 0.95 cc/g with an increase in Pd content while no distinct trend in surface area with Pd content was observed. The pore size was found to decrease as the Pd loadings increased. For the post impregnation series, the 1%-Pd-MCM-48-A-Tol-PI prepared using $Pd(acac)_2$ in toluene exhibited the highest surface area of 1360 m^2/g and pore volume of 0.68 cc/g.

3.4. Transmission electron microscopy studies

Transmission electron microscopic studies were carried out to confirm the cubic phase of Pd-MCM-48 materials. Fig. 9 shows representative TEM image for 1%Pd-MCM-48-D-N01 prepared using Pd(0) nanoparticles that were reduced by 0.1 N $NaBH_4$. The TEM image along the [1 1 0] axis clearly indicate the bi-continuous pore system consistent with previously published results. Careful and close examination of the TEM image indicates that the Pd nanoparticle is fairly distributed uniformly. As the TEM images indicate, most of the Pd particles (<2 nm) are located inside the pores of MCM-48, while some particles (in the 4–7 nm range) are located outside the mesopores. The larger Pd particles have sintered to form larger clusters after calcination and reduction and in order to estimate the average Pd crystallite sizes, CO chemisorption studies were carried out.

3.5. CO pulse chemisorption studies

CO pulse studies are valuable in determining Pd metal crystallite size, surface area and dispersion. With this purpose, we performed CO chemisorption at room temperature for several Pd containing MCM-48 materials. Table 3 shows the results obtained for samples that were prepared using the various methods. The different metal loading for 1, 2, 3, and 4%Pd-MCM-48-D-N01 prepared using Pd(0) nanoparticles and reduced with 0.1 N $NaBH_4$, were also compared in this study. Here, an increase in the Pd metal loading resulted in an increase in the Pd crystallite size from 5 to 60 nm as well as a corresponding decrease in the Pd dispersion from 21.4% to 1.9%. It is noteworthy to point out that the sample 1%Pd-MCM-48-D-N01 showed a relatively high dispersion of 21.4%. This is significantly higher than an earlier reported dispersion value of 3.3 [12] for similar Pd loading level. At a similar Pd(0) nanoparticle loading of 1 wt.%, an increase in the

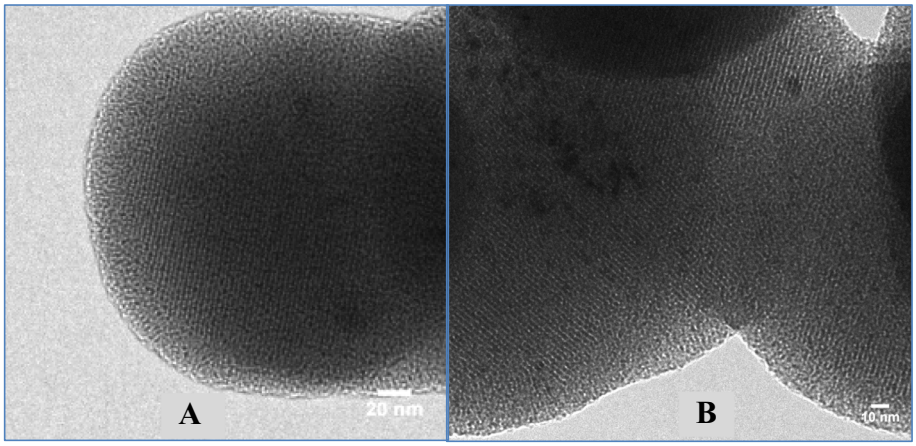

Fig. 9. Representative transmission electron microscopic images of 1%Pd-MCM-48-D-N01 with magnification of (A) 20 nm and (B) 10 nm.

Table 3
CO pulse studies over different metal loaded Pd-MCM-48 at room temperature.

Material	Pd dispersion (%)	Pd crystallite size (nm)	Surface area/g of Pd (m^2/g)
1%Pd-MCM-48-D-N01	21.4	5	95.3
2%Pd-MCM-48-D-N01	7.9	14	35.4
3%Pd-MCM-48-D-N01	3.9	28	17.7
4%Pd-MCM-48-D-N01	1.9	60	8.3
1%Pd-MCM-48-D-N05	10.4	11	46.6
1%Pd-MCM-48-D-N1	2.9	38	12.9
1%Pd-MCM-48-NP-PI	12.6	9	56.3
1%Pd-MCM-48-D-N01-PI	2.8	39	12.8
1%Pd-MCM-48-A-Tol-PI	6.5	17	28.7

concentration of $NaBH_4$ reducing agent resulted in an increase in the crystallite size of Pd from 5 to 38 nm and a corresponding decrease in Pd dispersion from 21.4% to 2.9%. In the post impregnation series, a comparison of the use of different Pd precursors such as $Na_2[PdCl_4]$ (1%Pd-MCM-48-NP-PI), Pd(0) (sample labeled as 1%Pd-MCM-48-D-N01-PI) and Pd $(acac)_2$ (sample labelled as 1%Pd-MCM-48-A-Tol-PI) at the same loading of 1 wt.% revealed that Pd(0) nanoparticles are susceptible to greater agglomeration by the Pd(0)-DMAP encapsulation method as shown by the large Pd crystallite size of 39 nm in 1%Pd-MCM-48-D-N01-PI. It is worth mentioning that the CO chemisorption technique provides an estimate of the average crystallite sizes of Pd. The results also suggest that the dispersion of Pd varies depending on the preparative method.

3.6. Catalytic activity and recycling studies

Among the various methods examined in this study for the successful formation of cubic MCM-48 phase at room temperature, the method employing performed Pd(0) nanoparticles was the one that consistently and reliably formed the cubic phase. A representative sample that contains relatively large amounts of Pd dispersed on a cubic support was evaluated for catalytic studies. Thus, we used the catalyst, 3%Pd-MCM-48-D-N01 for exploring the hydrogenation of *trans*-cinnamic acid as a model reaction. The yield was found to be 100% after 30 min of reaction even after 6 cycles. AAS of the filtrate indicate absence of Pd indicating that the cubic MCM-48 support is a robust support for the dispersion of Pd(0) nanoparticles. It should be pointed out that all the samples, Pd-MCM-48-D-N01, containing 1, 2, 3, and 4 wt.% showed 100% yield after 30 min. The catalyst, 3%Pd-MCM-48-D-N01 had an impressive yield of 95% for hydrogenation of *trans*-cinnamic acid after 15 min of reaction whereas a commercial (Sigma–Aldrich) sample containing 10 wt.% of Pd/C showed gave only 25% yield under identical conditions.

Reusability is a crucial factor for evaluating the catalytic performance of heterogeneous catalysts. In this study, the material prepared using Pd(0) nanoparticles and reduced with 0.1 N $NaBH_4$ *i.e.* 3%Pd-MCM-48-D-N01 was recovered after the reaction and reused multiple times. Using hydrogenation of *trans*-cinnamic acid as a model reaction, the material was determined to be reusable with yields greater than 95% after 9 catalytic cycles as indicated in Table S1 in the Supplementary information. The recycling studies were also carried out without any loss in the quality of the cubic phase even after 6 cycles. The XRD patterns in Fig. S1 of the Supplementary information indicate that the cubic phase was retained after 6 cycles of hydrogenation. The surface area and pore volume of the spent (after 6 cycles) 3%Pd-MCM-48-D-N01 mesoporous material was found to be similar to the fresh sample. Also, CO chemisorption studies after 6 cycles indicate dispersion of Pd to be nearly 3.5%. Thus, the catalytic activity of 3%Pd-MCM-48-D-N01 after 6 cycles is similar to the fresh sample, since the dispersion of Pd, and the surface area and pore volume of the materials are similar and also due to the fact that the cubic phase is preserved. Additionally, the filtrate was analyzed for AAS and no Pd could be detected in the solution phase suggestion no leaching of Pd after 6 catalytic cycles. However, after the 7th cycle, there is some loss in the quality of the cubic phase since some of the peaks in 2θ region of 5–6° disappear suggesting a loss in the mesostructure. Also it appears that the cubic phase is completely destroyed after 9 catalytic cycles.

4. Conclusions

We have developed a synthetic procedure for the preparation of Pd-MCM-48 materials by a modified Stöber synthesis. The influences of varying the Pd precursors ($Pd(acac)_2$ and $Na_2[PdCl_4]$), and the time of addition of $Na_2[PdCl_4]$ on the formation of the cubic phase were investigated. When $Pd(acac)_2$ was used in preparation procedure, dissolving the Pd precursor is toluene media seemed more likely to form the cubic phase (albeit a poor one) whereas ethanol and water resulted in materials of the hexagonal and wormhole phases respectively. Alternatively, materials of wormhole, lamellar, and cubic phases were obtained when the $Na_2[PdCl_4]$ precursor was added at 20, 30 and 60 min after addition of all chemicals in the synthesis gel. In addition, it is more viable to prepare cubic Pd-MCM-48 at low loadings of <1 wt.% Pd using $Na_2[PdCl_4]$ at room temperature for 4 h. In the reduction of $Na_2[PdCl_4]$ to obtain Pd(0)-DMAP encapsulated nanoparticles, the

use of 0.1 and 0.5 N $NaBH_4$ resulted in cubic materials whereas the cubic phase was not preserved in increasing in concentration of the reducing agent to 1 N. Reusability studies assessing a material prepared using Pd(0)-DMAP encapsulated nanoparticles that were reduced with 0.1 N $NaBH_4$ *i.e.* 3%Pd-MCM-48-D-N01 indicate that the yields for the hydrogenation of *trans*-cinnamic acid are greater than 95% even after 8 catalytic cycles at which the cubic phase was maintained under our experimental conditions.

Acknowledgments

We extend sincere gratitude to NSF-CHE-0619190, NSF-CHE-0722632, NSF-CHE-0840507, NSF-EPS-0903804, DE-FG02-08ER64624, SD NASA EPSCoR NNX12AB17G and the State of South Dakota for funding this project. We also thank Dr. Ozan Ugurlu at the University of Minnesota Electron Microscopy Facility for providing assistance with TEM analyses.

Appendix A. Supplementary data

Supplementary data associated with this article can be found, in the online version, at http://dx.doi.org/10.1016/j.micromeso.2014.07.012.

References

[1] T. Wang, H. Kaper, M. Antonietti, B. Smarsly, Langmuir 23 (2006) 1489–1495.
[2] J.L. Bronkema, A.T. Bell, J. Phys. Chem. C 111 (2006) 420–430.
[3] B. Boote, H. Subramanian, K.T. Ranjit, Chem. Commun. (2007) 4543–4545.
[4] J.D. Revell, B. Dörner, P.D. White, A. Ganesan, Org. Lett. 7 (2005) 831–833.
[5] A. Sárkány, A. Horváth, A. Beck, Appl. Catal. A 229 (2002) 117–125.
[6] S.H. Joo, J.Y. Park, C.-K. Tsung, Y. Yamada, P. Yang, G.A. Somorjai, Nat. Mater. 8 (2009) 126–131.
[7] J.S. Choi, D.J. Kim, S.H. Chang, W.S. Ahn, Appl. Catal. A 254 (2003) 225–237.
[8] C. He, J. Li, J. Cheng, L. Li, P. Li, Z. Hao, Z.P. Xu, Ind. Eng. Chem. Res. 48 (2009) 6930–6936.
[9] P. Yang, Y. Shang, J. Yu, J. Wang, M. Zhang, T. Wu, J. Mol. Catal. A: Chem. 272 (2007) 75–83.
[10] K. Suzuki, S. Sato, M. Fujita, Nat. Chem. 2 (2010) 25–29.
[11] J. Demel, J. Čejka, P. Štěpnička, J. Mol. Catal. A: Chem. 274 (2007) 127–132.
[12] H.-Y. Lee, S. Ryu, H. Kang, Y.-W. Jun, J. Cheon, Chem. Commun. (2006) 1325–1327.
[13] A. Hammoudeh, S. Mahmoud, J. Mol. Catal. A: Chem. 203 (2003) 231–239.
[14] S. Banerjee, V. Balasanthiran, R.T. Koodali, G.A. Sereda, Org. Biomol. Chem. 8 (2010) 4316–4321.
[15] S. Banerjee, H. Khatri, V. Balasanthiran, R.T. Koodali, G. Sereda, Tetrahedron 67 (2011) 5717–5724.
[16] G.B. Xin, J.Z. Yang, W. Li, J. Zheng, X.G. Li, Eur. J. Inorg. Chem. (2012) 5722–5728.
[17] L.C. Wang, C.Y. Huang, C.Y. Chang, W.C. Lin, K.J. Chao, Microporous Mesoporous Mater. 110 (2008) 451–460.
[18] G. Alvez-Manoli, T.J. Pinnavaia, Z. Zhang, D.K. Lee, K. Marin-Astorga, P. Rodriguez, F. Imbert, P. Reyes, N. Marin-Astorga, Appl. Catal. A-Gen. 387 (2010) 26–34.
[19] C. He, J.J. Li, J. Cheng, L.D. Li, P. Li, Z.P. Hao, Z.P. Xu, Ind. Eng. Chem. Res. 48 (2009) 6930–6936.
[20] M. Chatterjee, A. Chatterjee, Y. Ikushima, Green Chem. 6 (2004) 114–118.
[21] K. Mukhopadhyay, B.R. Sarkar, R.V. Chaudhari, J. Am. Chem. Soc. 124 (2002) 9692–9693.
[22] B. Sarkar, R. Chaudhari, Catal. Surv. Asia 9 (2005) 193–205.
[23] T.T. Pham, S.P. Crossley, T. Sooknoi, L.L. Lobban, D.E. Resasco, R.G. Mallinson, Appl. Catal. A 379 (2010) 135–140.
[24] S. Liu, P. Cool, O. Collart, P. Van Der Voort, E.F. Vansant, O.I. Lebedev, G. Van Tendeloo, M. Jiang, J. Phys. Chem. B 107 (2003) 10405–10411.
[25] Y. Jiang, Q. Gao, J. Am. Chem. Soc. 128 (2005) 716–717.
[26] L.-C. Wang, C.-Y. Huang, C.-Y. Chang, W.-C. Lin, K.-J. Chao, Microporous Mesoporous Mater. 110 (2008) 451–460.
[27] W. Zhao, Q. Li, Chem. Mater. 15 (2003) 4160–4162.
[28] O. Mekasuwandumrong, S. Somboonthanakij, P. Praserthdam, J. Panpranot, Ind. Eng. Chem. Res. 48 (2009) 2819–2825.
[29] J. Panpranot, K. Pattamakomsan, P. Praserthdam, J.G. Goodwin, Ind. Eng. Chem. Res. 43 (2004) 6014–6020.
[30] M. Pedernera, O. de la Iglesia, R. Mallada, Z. Lin, J. Rocha, J. Coronas, J. Santamaría, J. Membr. Sci. 326 (2009) 137–144.
[31] J. Garcia-Martinez, N. Linares, S. Sinibaldi, E. Coronado, A. Ribera, Microporous Mesoporous Mater. 117 (2009) 170–177.